

Structural and Molecular Basis for Resistance to Aminoglycoside Antibiotics by the Adenylyltransferase ANT(2'')-Ia

Georgina Cox,^a Peter J. Stogios,^{b,c} Alexei Savchenko,^{b,c} Gerard D. Wright^a

Department of Biochemistry and Biomedical Sciences, Michael G. DeGroot Institute for Infectious Disease Research, McMaster University, Hamilton, Ontario, Canada^a; Department of Chemical Engineering and Applied Chemistry, University of Toronto, Toronto, Ontario, Canada^b; Center for Structural Genomics of Infectious Diseases (CSGID)^c†

† For this virtual institution, see <http://www.csgid.org>.

ABSTRACT The aminoglycosides are highly effective broad-spectrum antimicrobial agents. However, their efficacy is diminished due to enzyme-mediated covalent modification, which reduces affinity of the drug for the target ribosome. One of the most prevalent aminoglycoside resistance enzymes in Gram-negative pathogens is the adenylyltransferase ANT(2'')-Ia, which confers resistance to gentamicin, tobramycin, and kanamycin. Despite the importance of this enzyme in drug resistance, its structure and molecular mechanism have been elusive. This study describes the structural and mechanistic basis for adenylylation of aminoglycosides by the ANT(2'')-Ia enzyme. ANT(2'')-Ia confers resistance by magnesium-dependent transfer of a nucleoside monophosphate (AMP) to the 2''-hydroxyl of aminoglycoside substrates containing a 2-deoxystreptamine core. The catalyzed reaction follows a direct AMP transfer mechanism from ATP to the substrate antibiotic. Central to catalysis is the coordination of two Mg²⁺ ions, positioning of the modifiable substrate ring, and the presence of a catalytic base (Asp₈₆). Comparative structural analysis revealed that ANT(2'')-Ia has a two-domain structure with an N-terminal active-site architecture that is conserved among other antibiotic nucleotidyltransferases, including Lnu(A), LinB, ANT(4')-Ia, ANT(4'')-Ib, and ANT(6)-Ia. There is also similarity between the nucleotidyltransferase fold of ANT(2'')-Ia and DNA polymerase β. This similarity is consistent with evolution from a common ancestor, with the nucleotidyltransferase fold having adapted for activity against chemically distinct molecules.

IMPORTANCE To successfully manage the threat associated with multidrug-resistant infectious diseases, innovative therapeutic strategies need to be developed. One such approach involves the enhancement or potentiation of existing antibiotics against resistant strains of bacteria. The reduction in clinical usefulness of the aminoglycosides is a particular problem among Gram-negative human pathogens, since there are very few therapeutic options for infections caused by these organisms. In order to successfully circumvent or inhibit the activity of aminoglycoside-modifying enzymes, and to thus rejuvenate the activity of the aminoglycoside antibiotics against Gram-negative pathogens, structural and mechanistic information is crucial. This study reveals the structure of a clinically prevalent aminoglycoside resistance enzyme [ANT(2'')-Ia] and depicts the molecular basis underlying modification of antibiotic substrates. Combined, these findings provide the groundwork for the development of broad-spectrum inhibitors against antibiotic nucleotidyltransferases.

Received 23 October 2014 Accepted 2 December 2014 Published 6 January 2015

Citation Cox G, Stogios PJ, Savchenko A, Wright GD. 2015. Structural and molecular basis for resistance to aminoglycoside antibiotics by the adenylyltransferase ANT(2'')-Ia. *mBio* 6(1):e02180-14. doi:10.1128/mBio.02180-14.

Editor Karen Bush, Indiana University Bloomington

Copyright © 2015 Cox et al. This is an open-access article distributed under the terms of the [Creative Commons Attribution-Noncommercial-ShareAlike 3.0 Unported license](https://creativecommons.org/licenses/by-nc-sa/4.0/), which permits unrestricted noncommercial use, distribution, and reproduction in any medium, provided the original author and source are credited.

Address correspondence to Gerard D. Wright, wrightge@mcmaster.ca.

This article is a direct contribution from a Fellow of the American Academy of Microbiology.

The use of antibiotics for the successful treatment of infectious diseases has been severely compromised due to the emergence of multidrug-resistant bacteria, a problem that has been acknowledged on a global scale (1, 2). One class of antibiotics whose clinical efficacy is particularly diminished due to an increase in the prevalence of resistant bacteria is the aminoglycosides. The aminoglycosides are natural antibiotics produced from soil-dwelling bacteria. The founding member of this family, streptomycin, was identified in 1944 (3) and was the result of an orchestrated effort to identify antibacterial agents from fermentation products of soil microbes (4). Following the discovery of streptomycin, numerous

additional aminoglycosides were identified and semisynthetic derivatives such as amikacin developed, resulting in >20 members of this class, many of which are effective antimicrobial drugs.

The aminoglycosides are structurally diverse and consist of two or more amino-modified sugars linked to an aminocyclitol core; broad-spectrum bactericidal activity is achieved by interference with protein synthesis, including corruption of the genetic code (5). All members of this class bind to rRNA and proteins within the 30S subunit of the ribosome; however, interaction with and binding to the target are achieved in different ways according to the chemical structure of the drug (5).

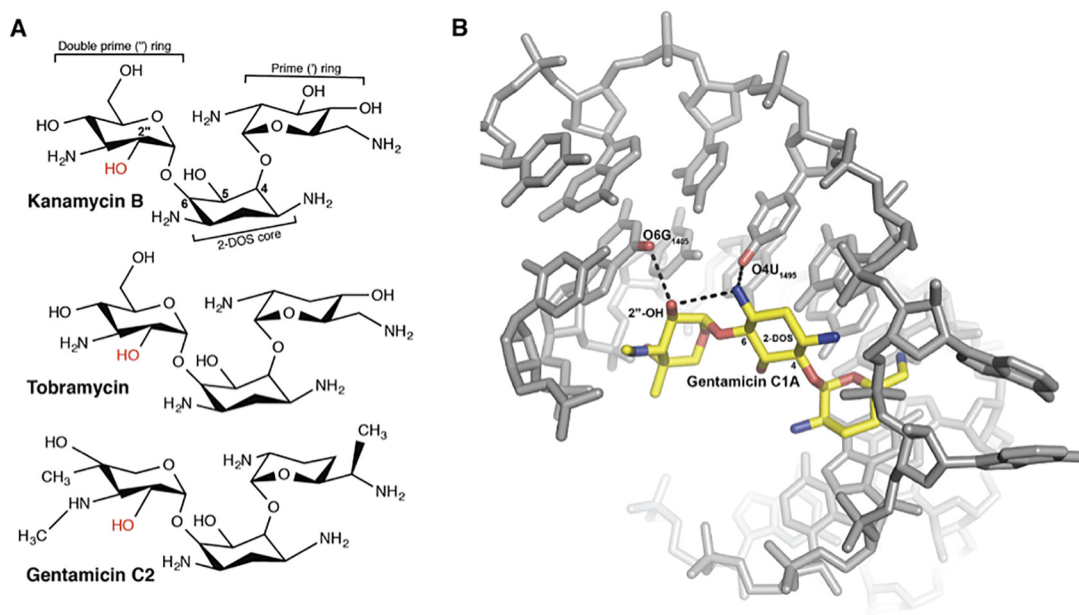


FIG 1 (A) 2-DOS (4,6-disubstituted 2-deoxystreptamine)-based aminoglycoside antibiotics amenable to modification by the nucleotidyltransferase ANT(2'')-Ia (23); the 2''-OH site of modification is in red. (B) Crystal structure of gentamicin C1A (in yellow) in complex with a decoding A site oligonucleotide (in grey) (7). Hydrogen bonds between the 2''-OH of gentamicin and the RNA are shown as dashed lines.

Members of the aminoglycoside family that contain a 2-deoxystreptamine (2-DOS) core, such as gentamicin, kanamycin, and tobramycin (Fig. 1A), have been particularly effective against many Gram-negative bacterial pathogens. This class of aminoglycoside is decorated at positions 4 and 6 of the 2-DOS core with amino-modified sugars; these substituents are referred to as the prime and double-prime rings, respectively. Such 4,6-disubstituted aminoglycosides bind to 16S rRNA; in particular, the double-prime ring exhibits key interactions with G1405 of the 16S rRNA (Fig. 1B) (6, 7).

Despite the broad-spectrum activity and clinical success of these drugs, their usefulness in the control of bacterial infections has been overshadowed by the emergence of resistance. Indeed, these drugs are inactivated by a variety of resistance mechanisms. The most common mechanism is covalent modification of the drug, a process that renders the antibiotic unable to bind effectively to the ribosome and thus alleviates the drug-induced translation interference (8). Aminoglycoside inactivation is catalyzed by a plethora of aminoglycoside-modifying enzymes (AMEs) that operate by different molecular mechanisms, including phosphorylation (catalyzed by nucleoside triphosphate-dependent *O*-phosphotransferases [APHs]), acetylation (catalyzed by acyl-coenzyme A-dependent *N*-acetyltransferases [AACs]) and adenylation (catalyzed by nucleoside triphosphate-dependent *O*-nucleotidyltransferases [ANTs]) (9).

Structural and biochemical knowledge of these modifying enzymes is crucial for the development of strategies to circumvent their activity and to thus rejuvenate the antibacterial action of the aminoglycosides (10). To date, there have been significant advances providing structural, mechanistic, and inhibitory insight into many members of the APH enzymes (11, 12). The AAC family has also been well characterized through structure-function studies of AAC(3) and AAC(6') enzymes (13–20). In contrast, the ANT family of enzymes is not well characterized (11), and there

are only three ANT enzymes with determined crystal structures: ANT(4')-Ia (PDB ID: 1KNY) (21), ANT(4')-IIb (PDB ID: 4EBJ and 4EBK), and ANT(6)-Ia (PDB ID: 2PBE).

There are five main classes of ANT enzymes, defined by their regioselectivity of chemical modification at positions 2'', 3'', 4'', 6, and 9 of substrate aminoglycosides. The aminoglycoside 2''-*O*-nucleotidyltransferase [ANT(2'')-Ia] was originally identified within a clinical isolate of *Klebsiella pneumoniae* in 1971 (22) and is now one of the most clinically prevalent ANT enzymes harbored by Gram-negative pathogens in North America (23–25). This allele has spread to many other bacterial genera, including *Pseudomonas*, *Acinetobacter*, and *Enterobacter*, all members of the so-called ESKAPE pathogens, which have been designated highly clinically important (26, 27).

ANT(2'')-Ia confers antibiotic resistance by magnesium-dependent transfer of a nucleoside monophosphate (AMP) to the 2''-OH of aminoglycoside substrates (Fig. 1A) (28). ANT(2'')-Ia is one of the few AMEs that modify a hydroxyl moiety on the double-prime ring. Understanding the molecular basis of ANT(2'')-Ia-mediated drug inactivation is vital to help guide the development of new aminoglycoside-like antibiotics such as plazomicin (29) and for the identification of inhibitors targeting AMEs, which could rescue the activity of older aminoglycoside drugs such as gentamicin. Here we report the three-dimensional (3D) structure of ANT(2'')-Ia and propose a molecular mechanism of adenylation mediated by this widespread resistance element.

RESULTS

Purification of ANT(2'')-Ia. Previous reports (30–34) indicated that expression of ANT(2'')-Ia in *Escherichia coli* resulted in only partially soluble recombinant protein. We expressed the enzyme in fusion with glutathione *S*-transferase (GST), which resulted in significant improvement in expression of soluble protein, allow-

TABLE 1 ANT(2'')-Ia steady-state kinetic parameters at 25°C

Enzyme and substrate	k_{cat} (s^{-1})	K_m (μM)	k_{cat}/K_m ($\text{M}^{-1} \text{s}^{-1}$)
Wild-type ANT(2'')-Ia; kanamycin B	5.2 ± 0.2	23.9 ± 6.6	2.1×10^5
Wild-type ANT(2'')-Ia; MgATP	15.3 ± 0.6	35 ± 7	4.4×10^5
D44A mutant; kanamycin B	<0.05		
D44A mutant; MgATP	<0.05		
D86A mutant; kanamycin B	<0.05		
D86A mutant; MgATP	<0.05		
H42A mutant; kanamycin B	<0.05		
H42A mutant; MgATP	<0.05		
R40A mutant; kanamycin B	7.5 ± 0.2	16.5 ± 1.6	4.53×10^5
R40A mutant; MgATP	8.1 ± 0.6	97 ± 14	8×10^4

ing us to obtain pure ANT(2'')-Ia (>95% homogeneity) after removal of the N-terminal GST moiety (see Materials and Methods). To confirm the activity of recombinant ANT(2'')-Ia, we used the EnzChek pyrophosphatase assay, which allows continuous measurement of the release of pyrophosphate by ANT(2'')-Ia by coupling it to the colorimetric detection of phosphate in the presence of excess pyrophosphatase. Accordingly, ANT(2'')-Ia kinetic parameters (Table 1) were consistent with previous reports (33), indicating that the protein retained full activity and was suitable for structural and mechanistic studies.

Structural characterization of ANT(2'')-Ia reveals the molecular framework for its activity. To decipher the mechanism underlying adenylation of 4,6-disubstituted 2-DOS-containing

aminoglycosides by ANT(2'')-Ia, we sought to determine the crystal structure of the protein alone and in complex with a substrate aminoglycoside. The apoenzyme structure was solved using the sulfur single-anomalous-dispersion (S-SAD) phasing method. The protein crystallized with one molecule per asymmetric unit, and the apo structure was refined to 1.48 Å. The ANT(2'')-Ia-kanamycin B cocrystal complex was solved by molecular replacement (MR) using the apoenzyme as the search model and refined to 1.73 Å. The final models of ANT(2'')-Ia contained interpretable electron density for residues 3 to 177 (refinement statistics can be found in Table 2).

The structure of ANT(2'')-Ia reveals that the protein comprises two main domains: a larger N-terminal domain (residues 3 to 92)

TABLE 2 X-ray diffraction data collection and refinement statistics

Statistic	Result for ligand (PDB code)	
	Apo (4WQK)	Kanamycin B (4WQL)
Data collection		
Space group	P2 ₁	P2 ₁
Cell dimensions		
<i>a</i> , <i>b</i> , <i>c</i> (Å)	45.5, 42.1, 47.7	45.5, 42.0, 47.8
β (°)	105.49	105.2
Resolution (Å)	40.0–1.48	25.0–1.73
R_{sym}^a	0.036 (0.251) ^b	0.064 (0.564)
$I/\sigma(I)$	63.68 (5.39)	33.4 (3.57)
Completeness (%)	96.8 (77.4)	100.0 (100.0)
Redundancy	7.0 (4.5)	4.4 (4.3)
Refinement		
Resolution (Å)	40.0–1.48	25.0–1.73
No. of unique reflections: working, test	28,068, 1,995	18,351, 1,781
<i>R</i> factor/free <i>R</i> factor ^c	15.9/19.6 (28.3/32.1)	14.8/18.4 (28.4/33.1)
No. of refined atoms (molecules)		
Protein	1415	1397
Magnesium	3	2
Substrate	NA	33
Other solvent	45	52
Water	281	243
<i>B</i> factors		
Protein	24.6	23.4
Magnesium	24.5	32.9
Substrate	NA	45.6
Other solvent	47.4	52.3
Water	39.2	40.7
RMSD		
Bond lengths (Å)	0.001	0.020
Bond angles (°)	1.441	1.668

^a $R_{\text{sym}} = \sum_i \sum_j |I_i(h) - \langle I(h) \rangle| / \sum_i \sum_j I_i(h)$, where $I_i(h)$ and $\langle I(h) \rangle$ are the *i*th and mean measurements of the intensity of reflection *h*.

^b Values in parentheses are those for the outer shells of the data.

^c $R = \sum |F_p^{\text{obs}} - F_p^{\text{calc}}| / \sum F_p^{\text{obs}}$, where F_p^{obs} and F_p^{calc} are the observed and calculated structure-factor amplitudes, respectively.

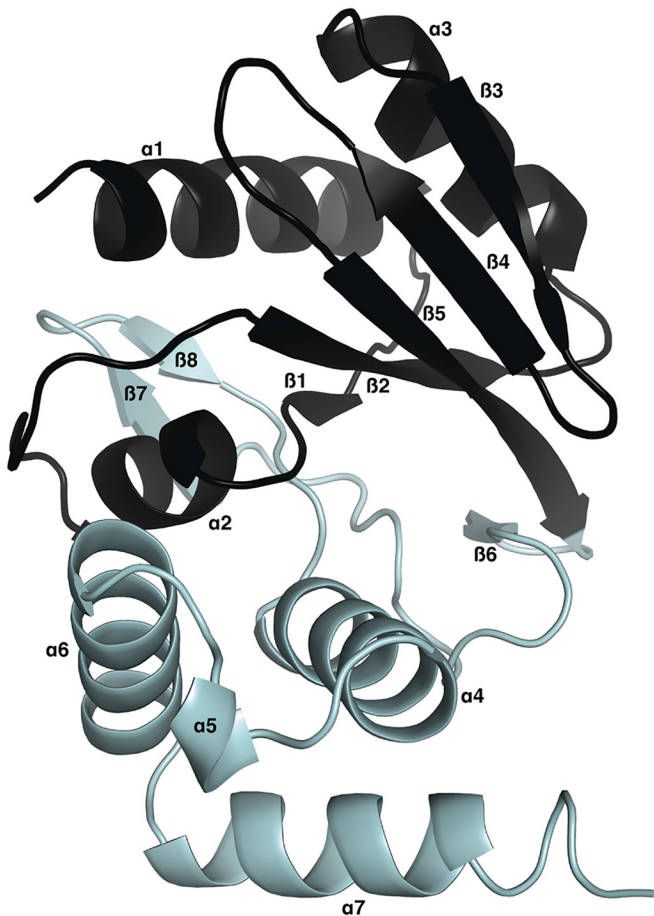


FIG 2 Crystal structure of ANT(2'')-Ia. The nucleotidyltransferase (NT) fold is in black, and the C-terminal domain is in cyan; α -helices and β -sheets are labeled.

that is centered on a β -sheet with three interspersed α -helices and a C-terminal domain (residues 93 to 177) that contains two β -hairpins followed by four α -helices forming a bundle (Fig. 2). The general conformation of the N-terminal domain of ANT(2'')-Ia (Fig. 2) follows the $\alpha 1$ - $\beta 1$ - $\alpha 2$ - $\beta 2$ -X- $\beta 4$ - $\beta 3$ NT fold topology (where X corresponds to a variable insert across nucleotidyltransferase [NT] fold-containing proteins), which is typical of this group of proteins (35). The C-terminal domain adopts two β -hairpins, with the first forming an interaction on one edge of the NT domain core β -sheet, plus a bundle of three α -helices.

ANT(2'')-Ia–kanamycin B complex structure reveals the specifics of antibiotic substrate recognition. The apo and kanamycin B-bound structures of ANT(2'')-Ia align with a root mean square deviation (RMSD) of 0.15 Å across 159 matching C α atoms, indicating that no gross conformational rearrangements occur upon aminoglycoside binding. The NT and C-terminal domains of ANT(2'')-Ia form the walls of a large cleft ~28 Å in diameter (Fig. 3A), which in the case of the kanamycin B-bound structure harbors unambiguous additional electron density corresponding to the antibiotic molecule. The central ring of the antibiotic is directed toward the interior of the protein, and the prime and double-prime rings point toward solvent (Fig. 3A and 4B). The cleft also harbors two Mg²⁺ ions; the first ion (Mg_I²⁺) is

coordinated by Asp₄₄ and Asp₄₆ and three ordered water molecules, whereas the second ion (Mg_{II}²⁺) is chelated by Asp₄₄, Asp₄₆, and Asp₈₆ side chains and the 2''-OH (the site of O-adenylation) and the 3''-NH₂ groups of the antibiotic substrate (Fig. 3B). Notably, both Mg²⁺ ions in the ANT(2'')-Ia active site lack a sixth coordinating ligand.

According to the ANT(2'')-Ia–kanamycin B complex structure, the antibiotic molecule is anchored in the enzyme active site through eight hydrogen bonds formed between side chain or main-chain atoms belonging to a total of nine residues (Fig. 3B). On the substrate side, hydrogen bonds are formed by the hydroxyl/amino groups that face the interior of the active site (Fig. 3B). Importantly, both the NT fold and the C-terminal domains of ANT(2'')-Ia contribute residues involved in binding the antibiotic substrate. The enzyme also forms two major stacking interactions between aromatic side chains and the antibiotic, with Tyr₇₄ and Tyr₁₃₄ situated over the central 2-DOS ring and the prime rings of kanamycin B, respectively. Electron density corresponding to the 6'' carbon and 6''-OH atoms of kanamycin B was relatively poorly defined, likely due to the lack of interactions between ANT(2'')-Ia and this area of the substrate. Overall, our analysis of the ANT(2'')-Ia–kanamycin B structure showed that the enzyme's active site forms interactions with all three rings of the aminoglycoside substrate. These interactions effectively secure the position of the 2''-OH nucleotidylation site in close proximity to the Mg_I²⁺ ion and the remainder of the deep active-site cleft, which is adequate in size to accommodate a nucleoside triphosphate (Fig. 3A).

ANT(2'')-Ia shares conserved molecular features with other NT-fold enzymes. Comparative structural analysis searches identified the lincosamide nucleotidyltransferase Lnu(A) (PDB ID: 4WH5 and 4FO1) as the closest structural homolog of ANT(2'')-Ia (Z score of 16.4), despite low primary sequence conservation between these enzymes (17% sequence identity). The ANT(2'')-Ia and Lnu(A) structures superposed with an RMSD of 2.4 Å over 146 C α atoms (Fig. 4A). However, Lnu(A) lacks an equivalent of the C-terminal α -helix in ANT(2'')-Ia (residues 166 to 177). Importantly, the similarity between these two enzymes extends to the molecular composition of their active sites, including the positions of the Mg²⁺-coordinating residues, which in both enzymes also coordinate the substrate antibiotic ring to be adenylated (Fig. 4B). In regard to the ANT(2'')-Ia–kanamycin B complex structure, the antibiotic appears to be more solvent exposed than lincomycin bound to Lnu(A); this observation is likely explained by the highly polar properties of the aminoglycosides. Furthermore, ANT(2'')-Ia residues conferring interactions with the antibiotic substrate are markedly different from their equivalents in Lnu(A).

We also observed significant structural similarity (Z score of 6.7 and C α RMSD of 3.4 Å across 109 matching C α atoms) between ANT(2'')-Ia and the lincosamide nucleotidyltransferase LinB (36), an enzyme that also features the NT fold domain (see Fig. S1 in the supplemental material). As observed between ANT(2'')-Ia and Lnu(A), residues of LinB coordinating the Mg²⁺ ions (Asp₄₀ and Asp₄₂) and the third acidic residue (Glu₈₉) are conserved (see Fig. S1); however, the C-terminal domains of ANT(2'')-Ia and LinB do not show any structural similarity.

Interestingly, our homology search also revealed similarity between the NT fold of ANT(2'')-Ia and DNA polymerase β (Pol β) (the palm domain) (37–39) (Fig. 4), a relationship that was also noted with ANT(4') (21). As we observed between ANT(2'')-Ia,

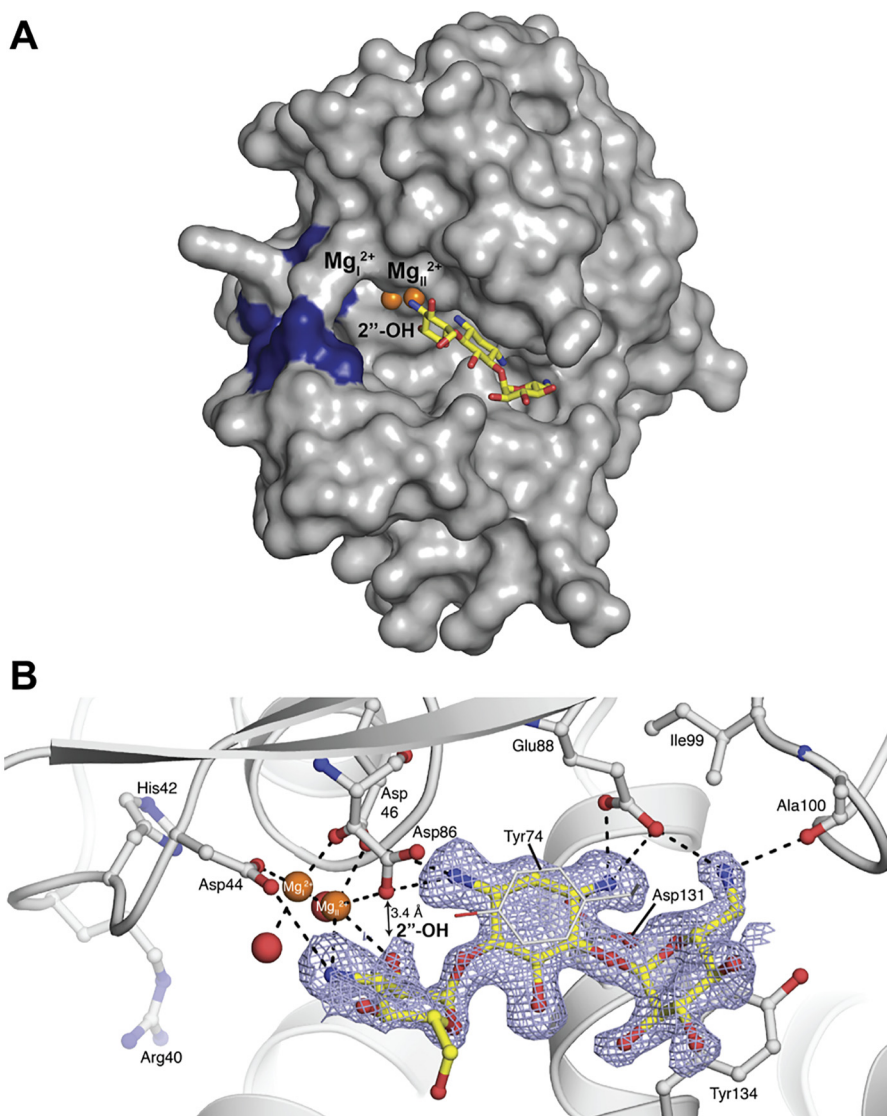


FIG 3 Molecular basis underlying adenylation of kanamycin B by ANT(2'')-Ia. (A) Surface representation of ANT(2'')-Ia with kanamycin B present in the large cleft. Catalytic Mg²⁺ ions are shown as orange spheres. The 2''-OH is also labeled and the region of the protein involved in nucleotide binding is in blue (the ternary structure of LinB [36] was used to assist in the identification of residues that may be important in nucleotide binding). (B) Interactions between the ANT(2'')-Ia active site and kanamycin B. The catalytic base is labeled (Asp₈₆), and bond distance (Å) between the 2''-OH of kanamycin B and Asp₈₆ is also shown. Electron density for kanamycin B is a simulated annealing F_o-F_c map contoured at 2.0 σ , and the Mg²⁺ ions are as described above.

Lnu(A), and LinB, the structural similarity with DNA Pol β extends to the architecture of the catalytic center (Fig. 4B). The three acidic residues, two Mg²⁺ ions, and position of the nucleotidyl-ation sites (3'-OH from the primer DNA for Pol β) spatially colocalize. In the polymerization reaction catalyzed by DNA Pol β , Asp₂₅₆ is considered the catalytic base that activates the primer DNA 3'-OH for nucleophilic attack on the α -phosphate of incoming nucleoside triphosphates (40). However, beyond this domain, DNA Pol β contains additional N- and C-terminal domains that do not share any structural similarity with ANT(2'')-Ia.

Finally, the structures of ANT(4')-Ia, ANT(4'')-IIb, and ANT(6)-Ia enzymes were also identified as ANT(2'')-Ia homologs that share the conserved NT fold. However, the orientation of the aminoglycoside substrates, the architecture of the C-terminal do-

main, and their oligomeric state (dimeric) differ dramatically from those of ANT(2'')-Ia.

Site-directed mutagenesis confirms individual roles of ANT(2'')-Ia active-site residues. To investigate the role of ANT(2'')-Ia active-site residues in catalysis and substrate recognition, we individually replaced them with alanine residues and tested the activities of corresponding enzyme variants *in vitro*. The Asp₄₄-to-Ala substitution resulted in complete loss of ANT(2'')-Ia activity against both kanamycin B and ATP, even at substrate concentrations 5 times the K_m (Table 1). Mutation of Asp₈₆ to Ala likewise rendered the enzyme entirely inactive (Table 1).

We attempted to determine a nucleoside triphosphate/analogous-bound complex structure of ANT(2'')-Ia but were not successful. Due to similarities in the active sites of LinB and

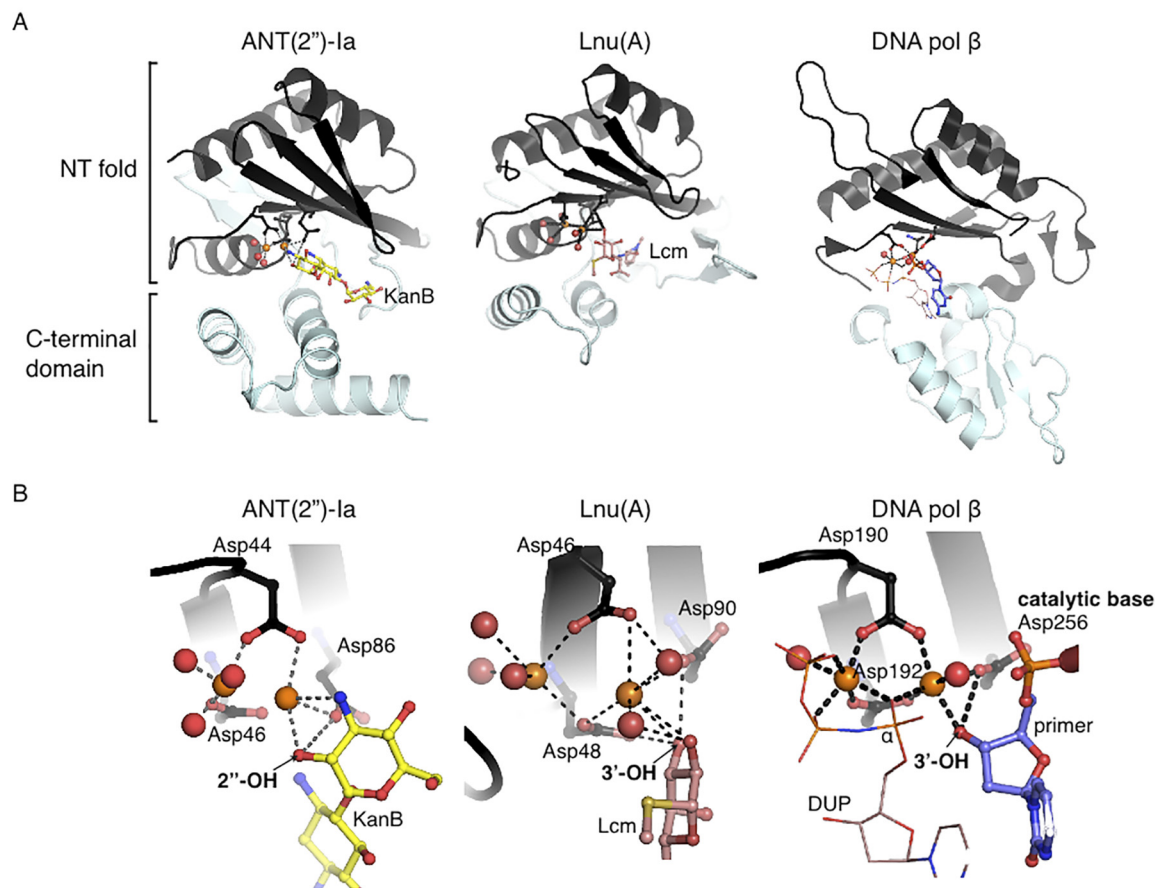


FIG 4 Conservation of the NT fold and catalytic architecture between ANT(2'')-Ia and nucleotidyltransferase enzymes. (A) Structures of ANT(2'')-Ia, lincosamide nucleotidyltransferase Lnu(A) (PDB ID: 4FO1), and DNA polymerase β (PDB ID: 2FMS) (37). The NT fold is in black, and the C-terminal domains are in light cyan. (B) Comparison of the catalytic architecture. Residues coordinating the Mg²⁺ ions are shown as sticks, Mg²⁺ ions and water molecules are shown as orange and red spheres, respectively, and dashed lines indicate hydrogen bonds. Kanamycin B (KanB), lincosamide (Lcm), and primer DNA are shown as sticks. DUP (2'-deoxyuridine-5'- α , β -imido-triphosphate) is shown as thin lines, and the α -phosphates are labeled. The modification site for each substrate is labeled.

ANT(2'')-Ia, the ternary structure of the former (36) was used to assist in the identification of residues that may be important in nucleotide binding. This comparison identified the positively charged residues Arg₄₀ and His₄₂ as likely candidates; indeed, replacement of His₄₂ resulted in loss of all enzyme activity (Table 1). However, Arg₄₀ only marginally reduced the nucleotidyltransferase activity. To ascertain the effect of Arg₄₀ substitution on nucleotide and kanamycin B binding, kinetic parameters were determined for both. For kanamycin B, the kinetics did not differ significantly from those of the wild-type enzyme, but nucleotide binding appeared to be impaired (Table 1). These findings implicate His₄₂ and Arg₄₀ in the function of ANT(2'')-Ia. Due to their distance from the kanamycin B 2''-OH group (10 and 13 Å, respectively), these residues are not involved in catalysis but instead likely coordinate ATP.

DISCUSSION

We present the structural and mechanistic characterization of the ANT(2'')-Ia enzyme in complex with its antibiotic substrate. The chemical modification of the 2''-OH provides the molecular logic for antibiotic resistance based on the importance of this site for interaction with the drug target (Fig. 1B) (28). Combining all of

our findings allows the proposal of a mechanism for adenylation by ANT(2'')-Ia (Fig. 5). The putative mechanism of ANT(2'')-Ia parallels the well-studied mechanism of DNA polymerization by DNA Pol β (40). Binding of the nucleoside triphosphate groups is stabilized by the two Mg²⁺ ions in the active site, His₄₂ and Arg₄₀, plus perhaps other nearby residues, such as Lys₁₄₇ and His₁₄₈. A catalytic base is predicted to be involved in a direct AMP transfer mechanism from ATP to the aminoglycoside, via activation of the 2''-OH. Our mutagenic and structural data suggest Asp₈₆ as a likely candidate, due to the fact that it is essential for catalysis and that its interactions with the 2''-OH of the aminoglycoside would provide electrophilic polarization, increasing the nucleophilicity of the alcohol. The interaction of Mg_{II}²⁺ with the substrate 2''-OH would also lend electrophilic polarization to this group. In general, this chemical environment feature is consistent with a nucleophilic attack on the α -phosphate of the nucleoside triphosphate by the substrate 2''-OH. Collapse of a tetrahedral intermediate would release the energetic pyrophosphate as a suitable leaving group.

Catalysis relies on coordination of Mg²⁺ ions, positioning of the substrate ring targeted for modification, and the presence of a catalytic base. We observed that these active-site residues are con-

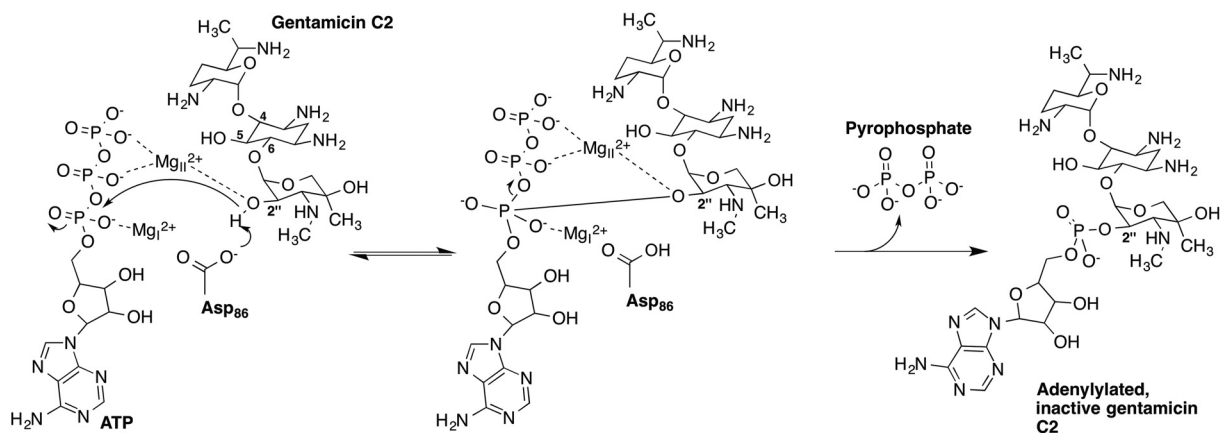


FIG 5 Magnesium dependent adenylation of gentamicin C2 by the aminoglycoside-modifying enzyme ANT(2'')-Ia.

served among other antibiotic nucleotidyltransferases, including Lnu(A), LinB, ANT(4')-Ia, ANT(4'')-Ib, and ANT(6)-Ia (36). The similarity of catalytic architecture among these enzymes with that of DNA Pol β , which was previously noted for LinB (36), is consistent with a shared catalytic mechanism utilized by these enzymes. In turn, these observations suggest an evolutionary relationship between ANT(2'')-Ia, Lnu(A), LinB, and DNA Pol β enzymes, with divergent evolution of the NT fold toward adaptation for activity against chemically distinct substrates. Clearly, substrate specificity dramatically differs and this diversification appears to be conferred by distinct C-terminal domains.

We anticipate that since ANT and Lnu enzymes share clear structural and catalytic similarities, as revealed through this study, it may be possible to develop broad-spectrum inhibitors against antibiotic nucleotidyltransferases. This strategy would rejuvenate multiple classes of antibiotics that are susceptible to inactivation via nucleotidylation. To allow for this possibility, it is necessary for these inhibitors to target the core nucleotidyltransferase catalytic machinery, since targeting the substrate recognition domain would be less fruitful. This study will allow such focused efforts, leading the way for structure-based drug design and the development of next-generation antibiotics that are recalcitrant to adenylation.

MATERIALS AND METHODS

Overexpression and purification of ANT(2'')-Ia. *E. coli* Rosetta (Merck KGaA, Darmstadt, Germany) (λ DE3; pDEST15:*aadB*) (*aadB*, GenBank no. ACX70191.1) was used for overexpression of ANT(2'')-Ia as a GST fusion product as previously described (41). Glutathione affinity chromatography was utilized as an initial purification step in buffer A (20 mM Tris [pH 8.0], 300 mM NaCl), and the GST fusion tag was removed by tobacco etch virus (TEV) protease cleavage at 12°C, followed by elution of the cleaved protein with buffer A. ANT(2'')-Ia was purified to high homogeneity (>95%) by the inclusion of a final purification step involving gel filtration chromatography. Separation was carried out at 4°C using a HiPrep S200 (26/60) prepacked column (GE Healthcare), and samples were eluted in buffer A (20 mM Tris [pH 8.0], 300 mM NaCl, 1 mM dithiothreitol [DTT], and 5 mM MgCl₂). For determination of the oligomeric state of ANT(2'')-Ia, the column was calibrated using a gel filtration LMW calibration kit (GE Healthcare) using the manufacturer's guidelines. ANT(2'')-Ia eluted as a single well-defined peak corresponding to a monomeric form and a molecular mass of ~20 kDa; accordingly, analysis of all crystal structure contacts using the PDBePISA server (42) did not reveal any oligomeric assemblies.

Crystallization of ANT(2'')-Ia and data collection. ANT(2'')-Ia was concentrated to 60 mg/ml, and crystals were grown at 20°C from hanging drops using the vapor diffusion method. Optimized crystallization conditions for ANT(2'')-Ia were 10% 2-propanol, 20% polyethylene glycol (PEG) 4000, and 0.1 M HEPES (pH 7.5). ANT(2'')-Ia was cocrystallized with kanamycin B (Sigma Aldrich, Oakville, ON, Canada) at a ratio of 5 times the molar concentration of the former. For data collection, the crystals were passaged through mother liquor containing 20% (vol/vol) glycerol and frozen in nitrogen.

Data were collected at 100 K with Cu K α X rays generated by a Rigaku 007 Microfocus rotating-anode generator equipped with VariMax HF optics and a Rigaku Raxis IV2+ detector. All X-ray data were reduced with HKL-3000 (43). The ANT(2'')-Ia apoenzyme structure was solved by S-SAD using Phenix.solve (44); four of the six sulfur sites (four cysteine residues) were located. Automated model building was performed with Phenix.autobuild, refinement was performed using Phenix.refine, and manual model building was performed with Coot (45). The ANT(2'')-Ia-kanamycin B complex structure was solved by molecular replacement (MR) using the apoenzyme structure. Fo-Fc difference density corresponding to the aminoglycoside molecule was readily traceable after MR. Translation-libration-screw rotation (TLS) parameterization was utilized for refinement of both structures. Geometries were verified using the Phenix and Coot validation tools and the RCSB PDB deposition server. Occupancy values for solvent molecules and Mg²⁺ atoms were refined. All B factors were refined as isotropic. Average B factor and bond angle/bond length RMSD values were calculated using Phenix.

Structure analysis. For comparison of similar structures, the C α RMSD was calculated using the SSM superposition tool in Coot (46) and the Dali server (47). The PDBePISA tool (42) was utilized to identify protein-ligand interactions. Structural homologs in the PDB were identified using the Dali server (47). Secondary structure boundaries were generated using the PDBsum server (48).

Site-directed mutagenesis. QuikChange (Agilent Technologies, Mississauga, Canada) site-directed mutagenesis was used to introduce point mutations within *aadB* in the pDEST15 vector (Life Technologies), according to the manufacturer's suggested guidelines. Primers were designed using the QuikChange primer design program (Agilent Technologies). Resulting mutants were confirmed by sequencing at the MOBIX Central Facility (McMaster University, Hamilton, Canada).

ANT(2'')-Ia steady-state kinetic studies. The continuous EnzChek pyrophosphate assay (Life Technologies) was used to assess wild-type and mutant ANT(2'')-Ia enzyme activity *in vitro*. The reaction was followed at 360 nm using a Spectramax Plus³⁸⁴ (Molecular Devices) microtiter plate reader. The assay was performed in duplicate, in 96-well plates (Nunc, ThermoScientific) with a final volume of 100 μ l and 50 mM HEPES [pH 7.5], 40 mM KCl, 10 mM MgCl₂, and 5 μ g of ANT(2'')-Ia. For char-

acterization of kanamycin B, ATP was kept at 5 times the K_m , and for assessment of ATP dependence, kanamycin was also kept at 5 times the K_m . The reaction mixtures were incubated with shaking for 3 min at 25°C, followed by initiation with nucleotide, and the formation of pyrophosphate was monitored for 10 min. Data were assessed using software in GraFit 5.0.13 (Erithacus Software).

SUPPLEMENTAL MATERIAL

Supplemental material for this article may be found at <http://mbio.asm.org/lookup/suppl/doi:10.1128/mBio.02180-14/-/DCSupplemental>.

Figure S1, PNG file, 0.4 MB.

ACKNOWLEDGMENTS

This work was supported by the Canadian Institutes of Health Research (MT-13536 to G.D.W.) and the Canada Research Chairs program (G.D.W.). The structures presented were solved by the Center for Structural Genomics of Infectious Diseases (CSGID; <http://csgid.org>); this project was funded in whole or in part with U.S. federal funds from the National Institute of Allergy and Infectious Diseases, National Institutes of Health, Department of Health and Human Services, under contract no. HHSN272200700058C (2007 to 27 September 2012) and HHSN272201200026C (starting 1 September 2012).

REFERENCES

- CDC. 2013. Antibiotic resistance threats in the United States. Centers for Disease Control and Prevention, Atlanta, GA.
- WHO. 2014. Antimicrobial resistance. Fact sheet no. 194. World Health Organization, Geneva, Switzerland.
- Schatz A, Bugle E, Waksman SA. 1944. Streptomycin, a substance exhibiting antibiotic activity against Gram-positive and Gram-negative bacteria. *Proc Soc Exp Biol Med* 55:66–69. <http://dx.doi.org/10.3181/00379727-55-14461>.
- Waksman SA. 1944. Antibiotic substances, production by microorganisms—nature and mode of action. *Am J Public Health Nations Health* 34:358–364. <http://dx.doi.org/10.2105/AJPH.34.4.358>.
- Magnet S, Blanchard JS. 2005. Molecular insights into aminoglycoside action and resistance. *Chem Rev* 105:477–498.
- Yoshizawa S, Fourmy D, Puglisi JD. 1998. Structural origins of gentamicin antibiotic action. *EMBO J* 17:6437–6448. <http://dx.doi.org/10.1093/emboj/17.22.6437>.
- François B, Russell RJ, Murray JB, Aboul-ela F, Masquida B, Vicens Q, Westhof E. 2005. Crystal structures of complexes between aminoglycosides and decoding A site oligonucleotides: role of the number of rings and positive charges in the specific binding leading to miscoding. *Nucleic Acids Res* 33:5677–5690. <http://dx.doi.org/10.1093/nar/gki862>.
- Wright GD. 2011. Molecular mechanisms of antibiotic resistance. *Chem Commun* 47:4055–4061. <http://dx.doi.org/10.1039/c0cc05111j>.
- Ramirez MS, Tolmasky ME. 2010. Aminoglycoside modifying enzymes. *Drug Resist Update* 13:151–171. <http://dx.doi.org/10.1016/j.drug.2010.08.003>.
- Stogios PJ, Spanogiannopoulos P, Evdokimova E, Egorova O, Shakya T, Todorovic N, Capretta A, Wright GD, Savchenko A. 2013. Structure-guided optimization of protein kinase inhibitors reverses aminoglycoside antibiotic resistance. *Biochem J* 454:191–200. <http://dx.doi.org/10.1042/BJ20130317>.
- Labby KJ, Garneau-Tsodikova S. 2013. Strategies to overcome the action of aminoglycoside-modifying enzymes for treating resistant bacterial infections. *Future Med Chem* 5:1285–1309. <http://dx.doi.org/10.4155/fmc.13.80>.
- Shakya T, Stogios PJ, Waglehner N, Evdokimova E, Ejim L, Blanchard JE, McArthur AG, Savchenko A, Wright GD. 2011. A small molecule discrimination map of the antibiotic resistance kinome. *Chem Biol* 18:1591–1601. <http://dx.doi.org/10.1016/j.chembiol.2011.10.018>.
- Wolf E, Vassilev A, Makino Y, Sali A, Nakatani Y, Burley SK. 1998. Crystal structure of a GCN5-related N-acetyltransferase: *Serratia marcescens* aminoglycoside 3-N-acetyltransferase. *Cell* 94:439–449. [http://dx.doi.org/10.1016/S0092-8674\(00\)81585-8](http://dx.doi.org/10.1016/S0092-8674(00)81585-8).
- Klimecka MM, Chruszcz M, Font J, Skarina T, Shumilin I, Onoprienko O, Porebski PJ, Cymborowski M, Zimmerman MD, Hasse-nyan J, Glomski IJ, Lebioda L, Savchenko A, Edwards A, Minor W. 2011. Structural analysis of a putative aminoglycoside N-acetyltransferase from *Bacillus anthracis*. *J Mol Biol* 410:411–423. <http://dx.doi.org/10.1016/j.jmb.2011.04.076>.
- Vetting MW, Hegde SS, Javid-Majd F, Blanchard JS, Roderick SL. 2002. Aminoglycoside 2'-N-acetyltransferase from *Mycobacterium tuberculosis* in complex with coenzyme A and aminoglycoside substrates. *Nat Struct Biol* 9:653–658. <http://dx.doi.org/10.1038/nsb830>.
- Vetting MW, Park CH, Hegde SS, Jacoby GA, Hooper DC, Blanchard JS. 2008. Mechanistic and structural analysis of aminoglycoside N-acetyltransferase AAC(6')-Ib and its bifunctional, fluoroquinolone-active AAC(6')-Ib-cr variant. *Biochemistry* 47:9825–9835. <http://dx.doi.org/10.1021/bi800664x>.
- Wybenga-Groot LE, Draker K, Wright GD, Berghuis AM. 1999. Crystal structure of an aminoglycoside 6'-N-acetyltransferase: defining the GCN5-related N-acetyltransferase superfamily fold. *Structure* 7:497–507. [http://dx.doi.org/10.1016/S0969-2126\(99\)80066-5](http://dx.doi.org/10.1016/S0969-2126(99)80066-5).
- Burk DL, Ghuman N, Wybenga-Groot LE, Berghuis AM. 2003. X-ray structure of the AAC(6')-Ii antibiotic resistance enzyme at 1.8-Å resolution; examination of oligomeric arrangements in GNAT superfamily members. *Protein Sci* 12:426–437. <http://dx.doi.org/10.1110/ps.0233503>.
- Burk DL, Xiong B, Breitbach C, Berghuis AM. 2005. Structures of aminoglycoside acetyltransferase AAC(6')-Ii in a novel crystal form: structural and normal-mode analyses. *Acta Crystallogr D Biol Crystallogr* 61:1273–1279. <http://dx.doi.org/10.1107/S0907444905021487>.
- Vetting MW, Vetting MW, Magnet S, Nieves E, Roderick SL, Blanchard JS. 2004. A bacterial acetyltransferase capable of regioselective N-acetylation of antibiotics and histones. *Chem Biol* 11:565–573. <http://dx.doi.org/10.1016/j.chembiol.2004.03.017>.
- Pedersen LC, Benning MM, Holden HM. 1995. Structural investigation of the antibiotic and ATP-binding sites in kanamycin nucleotidyltransferase. *Biochemistry* 34:13305–13311. <http://dx.doi.org/10.1021/bi00041a005>.
- Benveniste R, Davies J. 1971. R-factor mediated gentamicin resistance: a new enzyme which modifies aminoglycoside antibiotics. *FEBS Lett* 14:293–296. [http://dx.doi.org/10.1016/0014-5793\(71\)80282-X](http://dx.doi.org/10.1016/0014-5793(71)80282-X).
- Shaw KJ, Rather PN, Hare RS, Miller GH. 1993. Molecular genetics of aminoglycoside resistance genes and familial relationships of the aminoglycoside-modifying enzymes. *Microbiol Rev* 57:138–163.
- Shimizu K, Kumada T, Hsieh WC, Chung HY, Chong Y, Hare RS, Miller GH, Sabatelli FJ, Howard J. 1985. Comparison of aminoglycoside resistance patterns in Japan, Formosa, and Korea, Chile, and the United States. *Antimicrob Agents Chemother* 28:282–288. <http://dx.doi.org/10.1128/AAC.28.2.282>.
- Miller GH, Sabatelli FJ, Hare RS, Glupczynski Y, Mackey P, Shlaes D, Shimizu K, Shaw KJ. 1997. The most frequent aminoglycoside resistance mechanisms—changes with time and geographic area: a reflection of aminoglycoside usage patterns? Aminoglycoside Resistance Study Groups. *Clin Infect Dis* 24(Suppl 1):S46–S62. http://dx.doi.org/10.1093/clinids/24.Supplement_1.S46.
- Boucher HW, Talbot GH, Bradley JS, Edwards JE, Gilbert D, Rice LB, Scheld M, Spellberg B, Bartlett J. 2009. Bad bugs, no drugs: no ESCAPE! *Clin Infect Dis* 48:1–12. <http://dx.doi.org/10.1086/595011>.
- Pendleton JN, Gorman SP, Gilmore BF. 2013. Clinical relevance of the ESCAPE pathogens. *Expert Rev Anti Infect Ther* 11:297–308. <http://dx.doi.org/10.1586/eri.13.12>.
- Gates CA, Northrop DB. 1988. Substrate specificities and structure-activity relationships for the nucleotidylation of antibiotics catalyzed by aminoglycoside nucleotidyltransferase 2-I. *Biochemistry* 27:3820–3825. <http://dx.doi.org/10.1021/bi00410a045>.
- Endimiani A, Hujer KM, Hujer AM, Armstrong ES, Choudhary Y, Aggen JB, Bonomo RA. 2009. ACHN-490, a neoglycoside with potent in vitro activity against multidrug-resistant *Klebsiella pneumoniae* isolates. *Antimicrob Agents Chemother* 53:4504–4507. <http://dx.doi.org/10.1128/AAC.00556-09>.
- Bongaerts GP, Molendijk L. 1984. Relation between aminoglycoside 2"-O-nucleotidyltransferase activity and aminoglycoside resistance. *Antimicrob Agents Chemother* 25:234–237.
- Ekman DR, DiGiammarino EL, Wright E, Witter ED, Serpersu EH. 2001. Cloning, overexpression, and purification of aminoglycoside antibiotic nucleotidyltransferase (2")-Ia: conformational studies with bound substrates. *Biochemistry* 40:7017–7024. <http://dx.doi.org/10.1021/bi002827b>.

32. Smith AL, Smith DH. 1974. Gentamicin:adenine mononucleotide transferase: partial purification, characterization, and use in the clinical quantitation of gentamicin. *J Infect Dis* 129:391–401. <http://dx.doi.org/10.1093/infdis/129.4.391>.
33. Wright E, Serpersu EH. 2005. Enzyme-substrate interactions with an antibiotic resistance enzyme: aminoglycoside nucleotidyltransferase(2'')-Ia characterized by kinetic and thermodynamic methods. *Biochemistry* 44:11581–11591. <http://dx.doi.org/10.1021/bi050797c>.
34. Wright E, Serpersu EH. 2004. Isolation of aminoglycoside nucleotidyltransferase (2'')-Ia from inclusion bodies as active, monomeric enzyme. *Protein Expr Purif* 35:373–380. <http://dx.doi.org/10.1016/j.pep.2004.02.003>.
35. Kuchta K, Knizewski L, Wyrwicz LS, Rychlewski L, Ginalski K. 2009. Comprehensive classification of nucleotidyltransferase fold proteins: identification of novel families and their representatives in human. *Nucleic Acids Res* 37:7701–7714. <http://dx.doi.org/10.1093/nar/gkp854>.
36. Morar M, Bhullar K, Hughes DW, Junop M, Wright GD. 2009. Structure and mechanism of the lincosamide antibiotic adenylyltransferase LinB. *Structure* 17:1649–1659. <http://dx.doi.org/10.1016/j.str.2009.10.013>.
37. Batra VK, Beard WA, Shock DD, Krahn JM, Pedersen LC, Wilson SH. 2006. Magnesium-induced assembly of a complete DNA polymerase catalytic complex. *Structure* 14:757–766. <http://dx.doi.org/10.1016/j.str.2006.01.011>.
38. Davies JF, II, Almasy RJ, Hostomska Z, Ferre RA, Hostomsky Z. 1994. 2.3 Å crystal structure of the catalytic domain of DNA polymerase beta. *Cell* 76:1123–1133. [http://dx.doi.org/10.1016/0092-8674\(94\)90388-3](http://dx.doi.org/10.1016/0092-8674(94)90388-3).
39. Holm L, Sander C. 1995. DNA polymerase beta belongs to an ancient nucleotidyltransferase superfamily. *Trends Biochem Sci* 20:345–347. [http://dx.doi.org/10.1016/S0968-0004\(00\)89071-4](http://dx.doi.org/10.1016/S0968-0004(00)89071-4).
40. Batra VK, Shock DD, Prasad R, Beard WA, Hou EW, Pedersen LC, Sayer JM, Yagi H, Kumar S, Jerina DM, Wilson SH. 2006. Structure of DNA polymerase beta with a benzo[c]phenanthrene diol epoxide-adducted template exhibits mutagenic features. *Proc Natl Acad Sci U S A* 103:17231–17236. <http://dx.doi.org/10.1073/pnas.0605069103>.
41. Hirsch DR, Cox G, D'Erasmus MP, Shakya T, Meck C, Mohd N, Wright GD, Murelli RP. 2014. Inhibition of the ANT(2'')-Ia resistance enzyme and rescue of aminoglycoside antibiotic activity by synthetic alpha-hydroxytropolones. *Bioorg Med Chem Lett* 24:4943–4947. <http://dx.doi.org/10.1016/j.bmcl.2014.09.037>.
42. Krissinel E, Henrick K. 2007. Inference of macromolecular assemblies from crystalline state. *J Mol Biol* 372:774–797. <http://dx.doi.org/10.1016/j.jmb.2007.05.022>.
43. Minor W, Cymborowski M, Otwinowski Z, Chruszcz M. 2006. HKL-3000: the integration of data reduction and structure solution—from diffraction images to an initial model in minutes. *Acta Crystallogr D Biol Crystallogr* 62:859–866. <http://dx.doi.org/10.1107/S0907444906019949>.
44. Adams PD, Afonine PV, Bunkóczi G, Chen VB, Davis IW, Echols N, Headd JJ, Hung LW, Kapral GJ, Grosse-Kunstleve RW, McCoy AJ, Moriarty NW, Oeffner R, Read RJ, Richardson DC, Richardson JS, Terwilliger TC, Zwart PH. 2010. PHENIX: a comprehensive python-based system for macromolecular structure solution. *Acta Crystallogr D Biol Crystallogr* 66:213–221. <http://dx.doi.org/10.1107/S0907444909052925>.
45. Emsley P, Cowtan K. 2004. Coot: model-building tools for molecular graphics. *Acta Crystallogr D Biol Crystallogr* 60:2126–2132. <http://dx.doi.org/10.1107/S0907444904019158>.
46. Krissinel E, Henrick K. 2004. Secondary-structure matching (SSM), a new tool for fast protein structure alignment in three dimensions. *Acta Crystallogr D Biol Crystallogr* 60:2256–2268. <http://dx.doi.org/10.1107/S0907444904026460>.
47. Holm L, Rosenström P. 2010. Dali server: conservation mapping in 3D. *Nucleic Acids Res* 38:W545–W549. <http://dx.doi.org/10.1093/nar/gkq366>.
48. Laskowski RA, Hutchinson EG, Michie AD, Wallace AC, Jones ML, Thornton JM. 1997. PDBsum: a Web-based database of summaries and analyses of all PDB structures. *Trends Biochem Sci* 22:488–490. [http://dx.doi.org/10.1016/S0968-0004\(97\)01140-7](http://dx.doi.org/10.1016/S0968-0004(97)01140-7).